Available online at www.sciencedirect.com
SCIENCE DIRECT
Polymer 46 (2005) 3363–3371
polymer
www.elsevier.com/locate/polymer

Viscoelastic properties of ternary in situ elastomer composites based on fluorocarbon, acrylic elastomers and thermotropic liquid crystalline polymer blends

E. Shivakumar[a], C.K. Das[a,*], E. Segal[b], M. Narkis[b]

[a]*Materials Science Centre, Indian Institute of Technology, Kharagpur 721302, India*
[b]*Chemical Engineering Department, Technion, Haifa 32000, Israel*

Received 4 October 2004; received in revised form 25 January 2005; accepted 10 February 2005
Available online 21 March 2005

Abstract

Dynamic mechanical analysis was performed to characterize the viscoelastic properties of binary and ternary blends of fluorocarbon elastomer (FKM), acrylic elastomer (ACM) and liquid crystalline polymer (LCP). The results showed that the storage and loss modulus of all the blends increased significantly with the weight percentage of the LCP. The glass transition temperature evaluated at the loss modulus peak, were in the range of −10–+5 °C for all the blends. The time temperature superposition principle was applied for the FKM/ACM and 20% LCP filled FKM/ACM blend in order to evaluate the changes in the viscoelastic properties of FKM/ACM blend by the addition of LCP. The Arrhenius and William–Landel–Ferry (WLF) equations were used to quantify the viscoelastic behaviour at the glass transition region. Both the blends exhibited a single relaxation, which is glass transition, observed as a peek in the loss modulus at 1 Hz. The glassy moduli of these two systems were found to be comparable, but the rubbery moduli of the LCP filled FKM/ACM was much higher than the LCP unfilled system. However, the viscoelastic behaviour of these two systems and their sensitivity to time temperature may be considered to be quite similar.

Keywords: Viscoelstic properties; Dynamic mechanical analysis; Liquid crystalline polymer

1. Introduction

Thermotropic liquid crystalline polymers (TLCPs) are a relatively new class of materials; they are under extensive investigation, which is still growing in scope. Many studies have been reported concerning their rheological, dielectric, thermal and mechanical properties, and processing and morphology [1–8]. New areas of their potential applications continue to emerge. The TLCPs have good physical and mechanical properties as well as better dimensional stability and chemical resistance than flexible polymers. They show easy of processing due to their low melt viscosity.

During the last few years, most attention has been paid to the blending of TLCPs with less expensive flexible polymers. Addition of TLCPs to such polymers not only enhances mechanical properties of the resulting composites obtained due to the orientation of the LCP phase, but also improves their processing properties. Even relatively small amount of a LCP may induce a reduction in the melt viscosity and thus improve the processability. In most cases, under appropriate processing conditions the dispersed phase can be deformed in to a fibrillar one. The resulting self-reinforced is hence some times called in situ composites. Many researchers have studied polymer blends in which one component is liquid crystalline in nature [8–11]. In general, these researchers have elucidated the rheological, mechanical, and morphological characteristics of such blends. Despite this large volume of results, there are almost no papers on the thermoviscoelastic behaviour of LCPs and their blends with elastomers. However, Brostow et al. [12] have studied the viscoelastic properties of LCP/PP blends and they have successfully applied time temperature superposition principle to creep and stress relaxation data of PP/LCP blends.

* Corresponding author. Tel.: +91 3222 283978; fax: +91 3222 255303.
E-mail address: ckd@matsc.iitkgp.ernet.in (C.K. Das).

0032-3861/$ - see front matter © 2005 Elsevier Ltd. All rights reserved.
doi:10.1016/j.polymer.2005.02.092

1.1. Time temperature superposition (TTS)

When dynamic mechanical measurements carried out over a fixed range of frequency at several temperatures, a series of isothermal curves (storage (E') and loss (E'') moduli, etc.) can be generated. For materials that follow the time temperature superposition principle (TTS) [13], these isothermal modulus curves can be superposed through horizontal and/or vertical shifts. The shifted curves result in a master curve, at a reference temperature, describing the viscoelastic behaviour of the materials for a wider range of frequencies, compared to the one used for each individual temperature [14]. TTS can also be used to describe the influence of temperature on rheological properties of polymers and as tool to obtain information on polymer branching [14], phase segregation in polymer blends [15], and glass transition [16]. Normally TTS does not hold for polymer blends because of the individual contribution of each phase to the rheological behaviour of the blend. However, if a successful compatibilization is achieved, i.e. strong interactions among the phases are prompted by the presence of block copolymers at the interface, a homogeneous rheological behaviour of the blend can be expected.

In order to understand the viscoelastic properties of pure and LCP filled blends, under oscillating forces, here first time we have utilized the time temperature superposition principle (TTS). In the present investigation we have studied the viscoelastic properties of fluorocarbon elastomer (FKM), polyacrylic rubber (ACM) and liquid crystalline polymer (LCP) blends. The investigated results are reported and discussed in this paper.

2. Experimental

2.1. Materials and preparation of blends

Fluorocarbon rubber (FKM) used was Viton E 60-C, by Du Pont (USA), Polyacrylic rubber (ACM) used was AR 31, Nippon Zeon (Japan) and LCP used was Vectra A950 from Ticona (USA). The curative used was 4,4′methylene-bis-(cyclohexylamine)-carbamate (Diak 4) (Du Pont, USA) along with hexamethylenetetramine (HMT) (Aldrich, India) and lead monoxide (PbO) (Qualigens, India). The code names and the compositions of the different samples under study are listed in Table 1. The mixing of LCP with FKM and FKM/ACM was done with the help of high temperature sigma internal mixer at 290 °C for 8 min with 100-rpm rotor speed. The blended compound was then mixed with Diak 4-HMT-PbO at 60 °C in two roll open mixing mill and vulcanized by compression molding up to an optimum cure time at 150 °C and 20 MPa. The dynamic mechanical properties were determined from the vulcanized slabs thus prepared.

Table 1
Blending formulations

Code name ↓	Blend composition[a]		
	FKM	ACM	LCP
L_0	100	–	0
L_1	80	–	20
L_2	60	–	40
L'_0	60	40	0
L'_1	48	32	20
L'_2	36	24	40

[a] All blends contain Diak 4, HMT, and PbO, 1.5, 0.5, and 2 phr, respectively, with respect to rubber content.

2.2. Apparatus and procedure

Dynamic mechanical properties of the blends were analysed using a TA Instrument DMA 2980 dynamic mechanical analyser under tension clamp. The results for two distinct types of mechanical tests are presented in this paper. For temperature sweeps, to measure the glass transition temperature (T_g) and dynamic mechanical properties, the samples were subjected to a sinusoidal displacement of about 0.1% strain at a frequency of 1 Hz from −50 to +150 °C and a temperature rate of 5 °C min^{-1}. For the master curve construction (frequency domain analysis), the samples were tested under isothermal conditions from 0.1 to 100 Hz. After the testing at a particular temperature was completed, the temperature was then stepped up 10 °C (taking less than 1 min), held isothermally for 5 min, and then the frequency scanning at the new test temperature conducted. This procedure was repeated until the final test temperature was reached. Fourier transform infrared spectroscopy (FTIR) experiments were done on thin films of ACM, FKM, LCP, and their blends using a NEXUS 870 FTIR (Thermo Nicolet) in humidity less atmosphere at room temperature. A total of 32 scans were averaged with a resolution of 4 cm^{-1}. Morphologies of the tensile fractured surfaces of the samples were examined using a JSM-5800 of JEOL Co. scanning electron microscope (SEM), after auto sputter coating of the fractured surface with gold at 0° tilt angle.

3. Results and discussion

3.1. Dynamic mechanical analysis (DMA)

Loss tangent (tan δ) of the binary and ternary blends as a function of temperature is shown in Fig. 1(a) and (b), respectively, and the corresponding parameters are given in Table 2. In Fig. 1(a), the FKM shows two loss peaks in the temperature range of −50–+150 °C, which have been labelled as α and T_α occurring at about 3 and 68 °C, respectively. For the FKM/ACM blend the α-peak was observed at 15 °C, which is nearly 12 °C higher than that of FKM, however the tan δ_{max} value is nearly same for the both

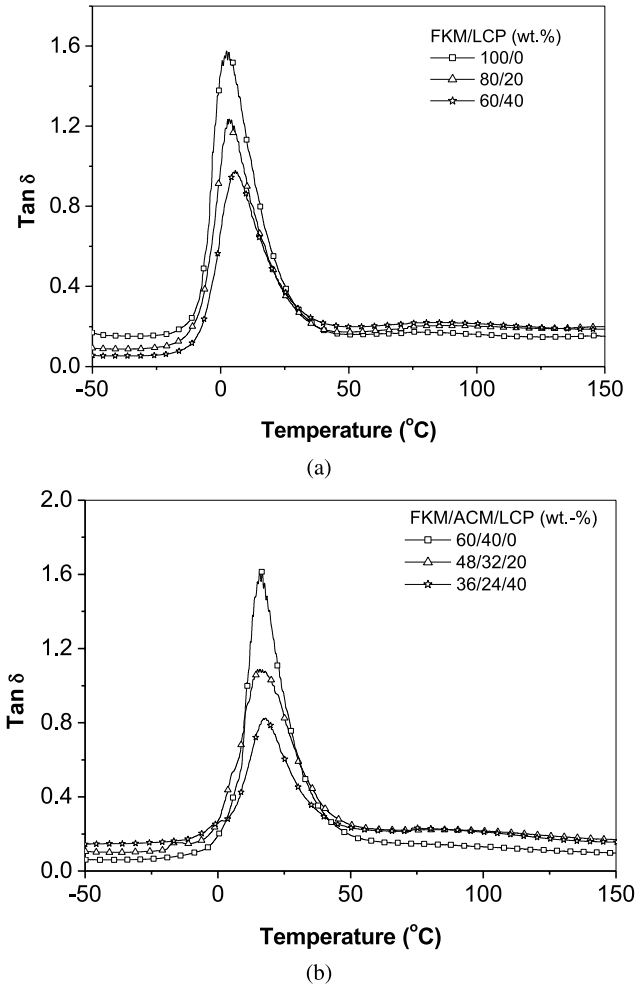

Fig. 1. Loss tangent (tan δ) as a function of temperature at 1 Hz frequency for (a) binary blends; (b) ternary blends.

FKM and FKM/ACM. Addition of 10% LCP to FKM, the α-peak shifted to higher temperature side and the tan δ_{max} decreased, these characteristics increased with the increasing LCP content. The same trend was observed for the ternary blends, however, the tan δ_{max} decreased at a higher rate in the case of ternary blends compared to binary blend system. This can be discussed in light of structural changes associated with the level of interaction between rubber and LCP phases. It is known that the height of the dynamic transition of a component of a composite apparently reflects the relative quantity of the component it self [17–19]. Also, the model calculations based on the modified Kerner equation and presented in detail by Dickie [20] indicated that the height of the dispersed phase loss peak is principally a function of inclusion volume fraction. Thus, it may be said that the decrease of tan δ_{max} of rubber in the blend is the result of a reduction of the relative quantity of bulk rubber in the dynamic transition. This explanation is quite reasonable for the decrease in the tan δ_{max} with the addition of LCP for both the binary and ternary blends, however, the decrease in tan δ_{max} is more predominant in the case of ternary blend even though the weight fraction of the rubber in binary and ternary blends are same for the different compositions of LCP (i.e. 20, 40% LCP), and also the tan δ_{max} value is nearly same for both FKM and FKM/ACM blend, this extent of reduction in tan δ_{max} of FKM/ACM by the addition of LCP may be interpreted as progressive immobilization of the rubber chains close to the boundary between two phases when they are increasingly grafted to the LCP phase. From this it can be concluded that the ACM enhances the interaction between FKM and LCP. As the temperature was increased, another relaxation was observed at about 68 °C. This peak is not clearly evident in Fig. 1 because of the supremacy of α-peak, after reducing the scale; the peak is clearly observed (Fig. 2). This relaxation was assumed to be melting of FKM crystallites as reported by Hoffmann [21]. Addition of LCP, the T_α peak of FKM appeared to be broader and slightly shifted to higher temperature side. This may be due to the melting of FKM crystals associated with the β transition of LCP. Since the β transition of LCP is 70 °C [22,23].

Plots of the storage modulus (E') versus temperature at 1 Hz for both the binary and ternary blends are shown in Fig. 3(a) and (b), respectively, together with those of pure FKM and FKM/ACM. It can be seen from the Fig. 3 that all the binary and ternary blends started to exhibit steep drop in glassy state storage modulus (E') value at their corresponding glass transition region, this is followed by a plateau. Addition of LCP is seen to increase the storage modulus at room temperature (i.e. 30 °C) and also the modulus in plateau is found to increase. This increase in the modulus of plateau is beneficial to ensure better high temperature performance of the blends. This could be attributed to the presence of LCP of high intrinsic modulus in the FKM matrix. The storage modulus of the binary and ternary

Table 2
Dynamic mechanical parameters of the binary and ternary blends

Sample code	E''_{max} (MPa)	T_g at E''_{max} (°C)	tan δ_{max}	$T_{\delta_{max}}$ (°C)	E' (MPa)		
					30 °C	100 °C	150 °C
L_0	265.4	−7.1	1.57	3.4	3.4	1.9	1.4
L_1	286.9	−4.1	1.24	3.2	6.5	2.6	1.6
L_2	338.7	−2.6	0.99	5.7	17.1	8.4	5.7
L'_0	223.0	3.0	1.58	15.9	4.5	1.4	1.1
L'_1	298.2	5.0	1.09	15.8	11.1	5.5	3.7
L'_2	305.5	5.2	0.82	18.1	24.3	10.4	7.2

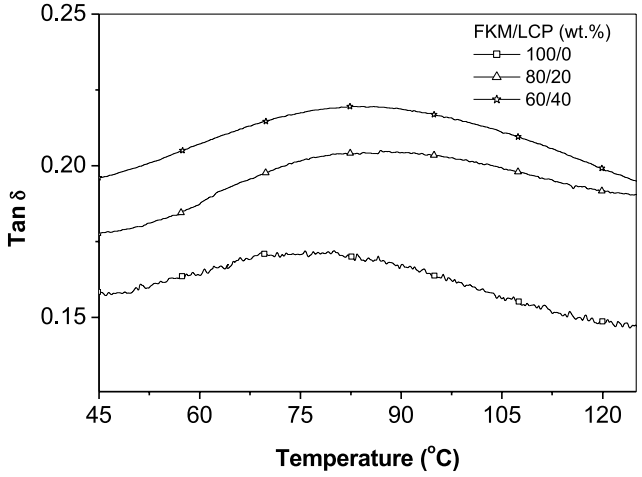

Fig. 2. Loss tangent (tan δ) as function of temperature at 1 Hz frequency for the FKM/LCP blends.

blends at different temperatures is given in Table 2. At three temperatures, the storage modulus of binary and ternary blends is found to increase with increasing LCP is an indication of reinforcement and can be attributed to be change in morphology. However, this increase in E' is more predominant in the case of ternary blend system, this extent of increase in E' is due to increase of interaction between FKM and LCP in presence of ACM. Similar observation has also been made by Weiss et al. [24] for different pairs of LCP thermoplastics. In order to give further support on the interaction between components of blends, the FTIR study has been carried out and the results were discussed briefly (the FTIR spectra are not given). The FTIR results showed a significant change at the C=O peak frequency of the pure ACM (1732 cm^{-1}) and LCP (1733 cm^{-1}) by blending these with FKM. The C=O peak of ACM in FKM/ACM blend was observed at 1724 cm^{-1}. The shift of the carbonyl-stretching peak to lower frequency due to FKM interaction as measured in the FTIR spectrum corresponds to negative heat of interaction [25]. Addition of 20% LCP to FKM/ACM, the C=O peak of the mixed ternary blend split in to two peaks, the peak at 1714 cm^{-1} is due to interaction with the FKM, the other peak observed at 1756 cm^{-1} is due to the formation of aromatic aliphatic ester linkages [26]. However, in FKM/LCP (80/20) blend the C=O peak of LCP was observed at 1731 cm^{-1}. This shift in C=O frequency of LCP in binary blend was very low when compared to ternary blend, so the ternary blend must have higher negative heat of interaction than the binary blend indicates strong interactions between the components of ternary blend due to the presence of ACM.

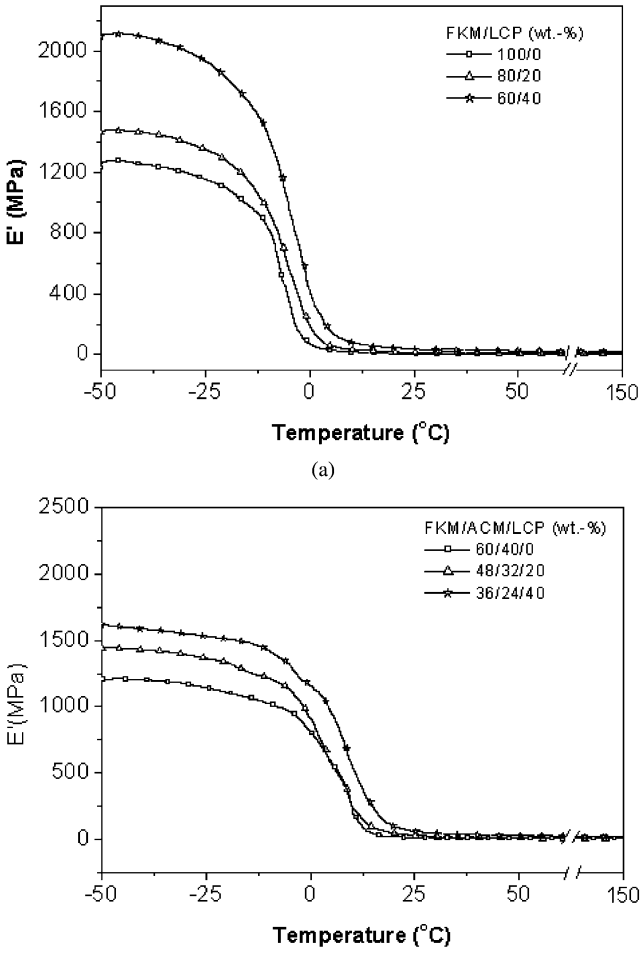

Fig. 3. Variation of the storage modulus (E') as a function of temperature at 1 Hz frequency for (a) binary blends; (b) ternary blends.

The loss modulus (E'') of the binary and ternary blends as a function of temperature is shown in Fig. 4(a) and (b). The T_g of the blends taken at the maximum of loss modulus and are shown in Table 2. FKM and FKM/ACM showed the T_g at −7 and +3 °C, respectively. Surprisingly the glass transition of LCP at 100 °C [27] was not observed. Similar observation also made by Das et al. [28] during their study on EPDM/LCP blends. The FKM/ACM showed sharp single peak representing single T_g, characteristic of miscible blends having homogeneous phase. It is observed from Fig. 4 that the increasing the LCP content in the binary and ternary blends the T_g slightly shifted towards higher temperature side due to decrease in flexibility of molecular chains as increasing the LCP content. Adding LCP in the blend, E'' at T_g is gradually increased for both the blend systems. Generally fibre filled elastomers shows much higher damping than unfilled elastomers [29]. This indicates that much of the energy must have dissipated in the LCP filled blends that may be at the elastomer, LCP interfaces, however, the E'' value in ternary blend increased at lower rate compared to that of binary blends. Overall the ternary blends showed lower damping (E'') than the binary blend system. This may be due to the increased interfacial adhesion between FKM and LCP in presence of ACM.

3.1.1. Time temperature superposition (TTS)

The superposition principle is based upon the premise that the processes involved in molecular relaxation or

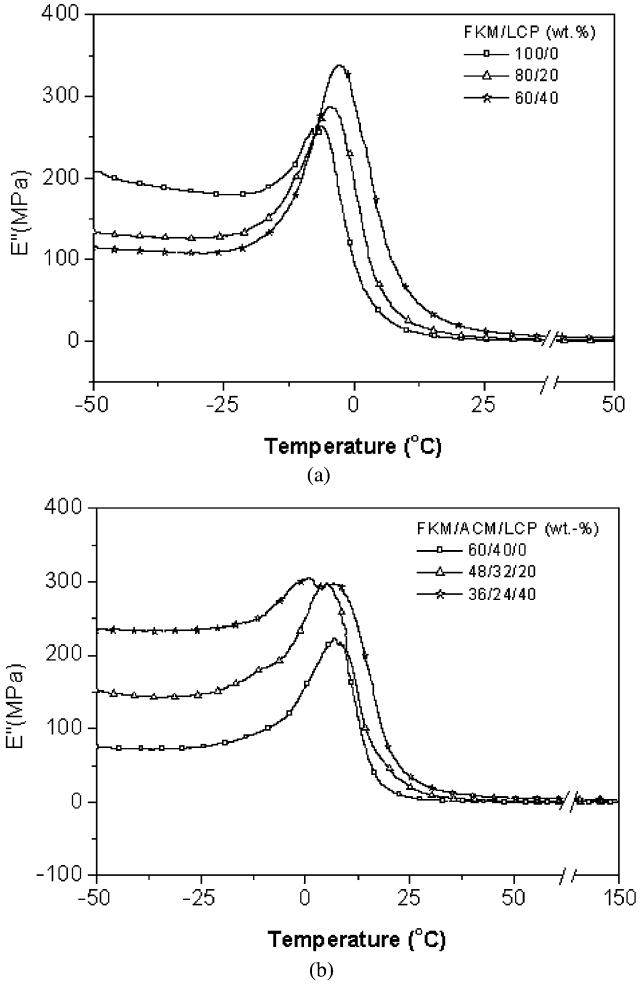

Fig. 4. Variation of the loss modulus (E'') as a function of temperature at 1 Hz frequency for (a) binary blends; (b) ternary blends.

rearrangements occurred at greater rates at higher temperatures [13]. The time over which these processes occurred could be reduced by conducting the measurement at elevated temperatures and transposing the data to lower temperatures. Thus, viscoelastic changes, which occurred relatively quickly at higher temperatures, can be made to appear as if they occurred at longer times or lower frequencies simply by shifting the data with respect to time (or frequency).

Fig. 5 shows the storage modulus data of FKM/ACM 60/40 (L'_0) blend, plotted on the log (E') − log (frequency) axes, with five segment curves, corresponding to the modulus data acquired at five equally spaced isothermal temperature steps between −10 and 30 °C. Each modulus curve consisted of 10 modulus data at the 10 frequencies (628–0.628 rad s^{-1} in logarithmic increments) scanned for each isothermal temperature. The reference curve was chosen as the modulus curve at 10 °C. Similarly, Fig. 6 shows the loss moduli data of the same sample on the log (E'') − log (frequency) axes.

Two master curves were generated by shifting the

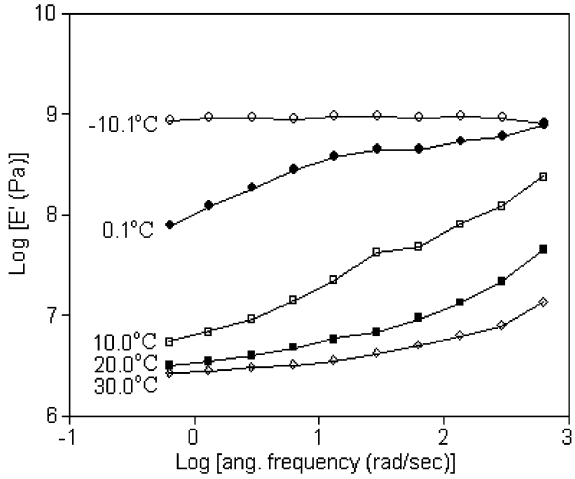

Fig. 5. Storage modulus of the FKM/ACM (60/40) sample at isothermal temperatures as a function of frequency plotted on the log–log scale.

storage and loss moduli curves, respectively, at different frequencies relative to the chosen reference curve. Fig. 7 shows the master curves by shifting both the storage and loss modulus data of sample L'_0 with the reference temperature chosen at 10 °C, respectively. These are called master curves because they shows the complete modulus versus time behaviour of a material at a constant temperature (reference temperature), which, coupled with a quantitative description of the shift factor versus temperature relationship, completely defines the viscoelastic properties of a material. The storage modulus master curve showed an elastic modulus of 1.02 GPa and rubbery modulus of 2.47 MPa. It is to be noted that the loss modulus master curve exhibited a maximum in the main viscoelastic region. The experimental data of the sample L'_0 indicated that the loss moduli approached non-zero values at the two extremes of low and high frequencies.

The time temperature superposition relationship usually is expected to hold only for thermorheologically simple

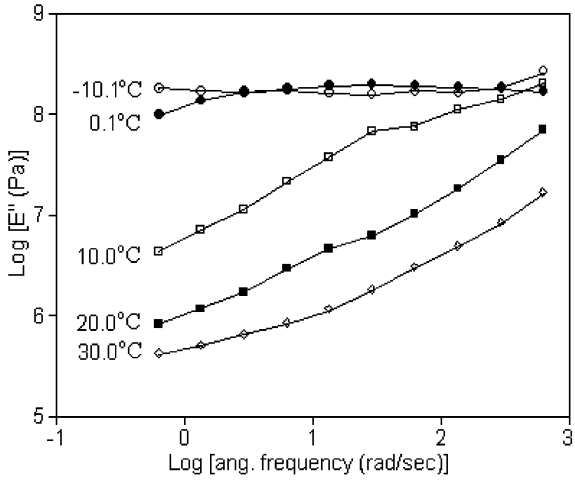

Fig. 6. Loss modulus of the FKM/ACM (60/40) sample at isothermal temperatures as a function of frequency plotted on the log–log scale.

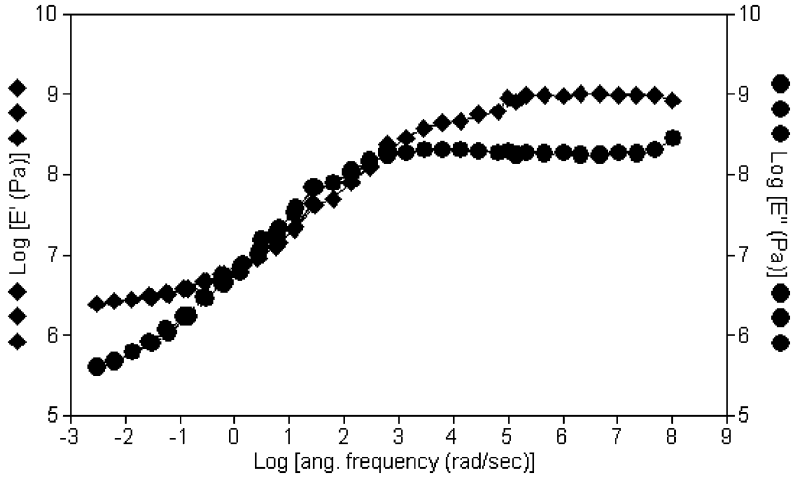

Fig. 7. Storage modulus and loss modulus of the FKM/ACM (60/40) blend as a function of frequency. Experimental data collected within a frequency range of 0.628–628 rad s^{-1} at different isothermal temperatures were shifted via time–temperature superposition to form a master reference curve at 10 °C.

materials. The ternary blend with 20%LCP (L'_1) was morphologically more complex than the L'_0 blend, as scanning electron microscope clearly indicated a complex morphology of L'_1 blend (Fig. 8). However dynamic mechanical analysis characterization performed on the L'_1 blend at 1 Hz did not suggest a multi phase structure (Fig. 4(b)). Therefore, although these materials were complex in compositions and morphology, the simple relaxation behaviour of L'_1 blend as revealed by the DMA results led us to assume a pseudo-homogeneous structure for the L'_1 sample to evaluate the viscoelastic properties of the blend using time temperature superposition principle. Time temperature superposition using WLF equation was similarly attempted to characterize the viscoelastic properties of the 20% LCP containing FKM/ACM blend.

Fig. 9 shows the storage modulus data of sample L'_1, plotted as a function of frequency, on a log (E')−log (frequency) plot. At five equally spaced isothermal temperatures between −10 and 30 °C. To generate a master curve, the temperature at 10 °C was chosen as the reference temperature, with respect to which other curves were shifted. Similarly Fig. 10 shows the loss moduli of sample

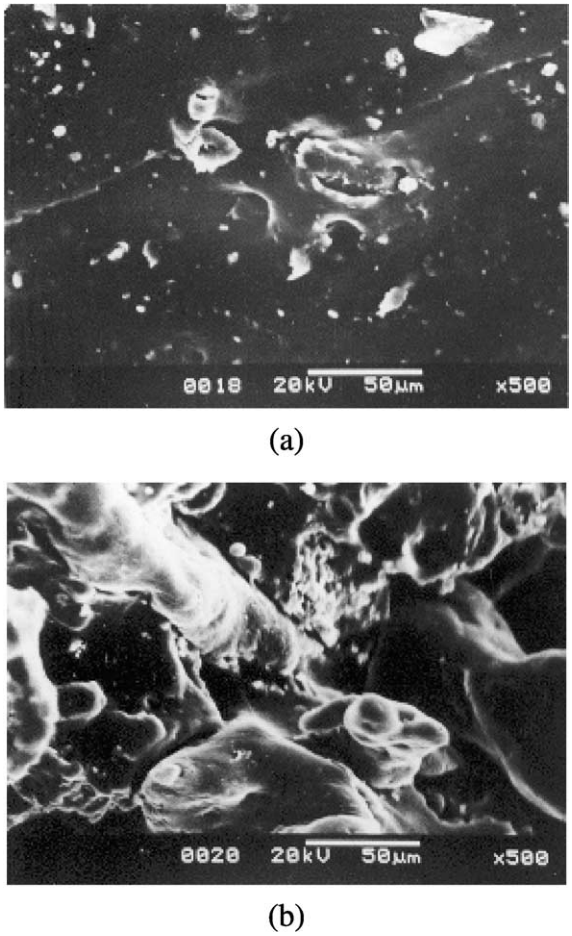

Fig. 8. SEM micrographs of fractured surfaces of (a) FKM/ACM (60/40); (b) 20% LCP filled FKM/ACM/LCP blends.

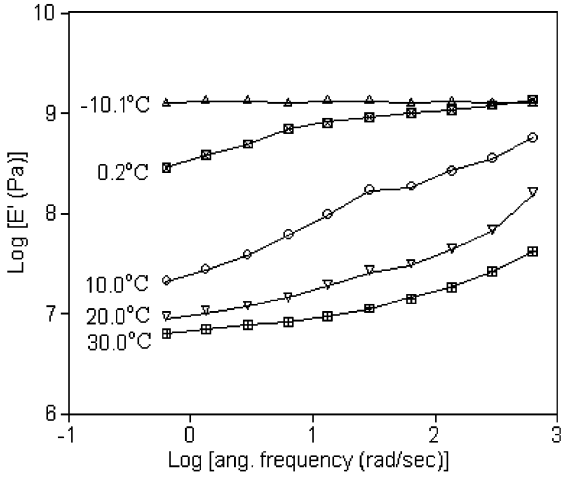

Fig. 9. Storage modulus of the 20% LCP filled FKM/ACM blend at isothermal temperatures as a function of frequency plotted on the log–log scale.

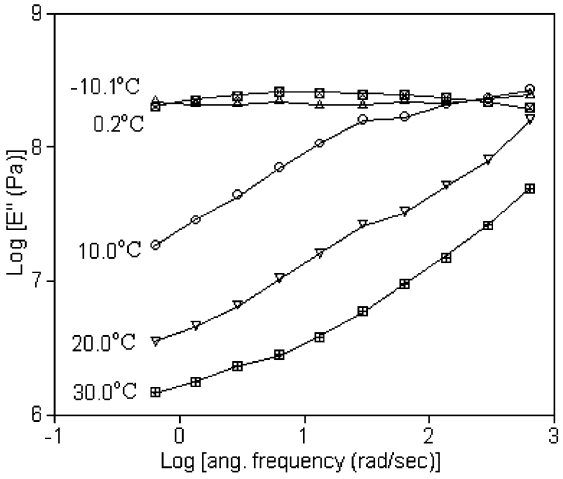

Fig. 10. Loss modulus of the 20% LCP filled FKM/ACM blend at isothermal temperatures as a function of frequency plotted on the log–log scale.

L'_1 are plotted as log [E''] − log [frequency] curves at five equally spaced isothermal temperatures from −10 to 30 °C.

Fig. 11 shows two master curves generated by shifting the storage and loss moduli curves, respectively, in the frequency domain with the reference temperature at 10 °C. The general viscoelastic behaviour of this L'_1 as revealed by the master curves was similar to that of L'_0 blend. The storage moduli (E') at long times (low frequencies) were lower, with a rubbery modulus of 6.01. The moduli at short times (high frequencies) were higher, with an elastic (glassy) modulus of 1.44 GPa. It is noted that the elastic moduli of the L'_1 blend was nearly 40% higher than the L'_0, where as rubbery moduli about 200% higher than that of the LCP unfilled system. The loss modulus master curve of this 20% LCP filled FKM/ACM ternary blend exhibited a maximum in the main viscoelastic transition, with general characteristics similar to those of the FKM/ACM blend system.

The calculated temperature dependence of shift factor (log a_T) fitted to the well-known William–Landel–Ferry (WLF) equation [13]:

$$\log a_T = \frac{-[C_1(T - T_0)]}{[C_2 + T - T_0]} \tag{1}$$

Where C_1 and C_2 are the WLF constants, T_0 the reference temperature and T measurement temperature.

Figs. 12 and 13 shows the shift factors, log a_T, obtained by shifting E' moduli as a function of temperature for L'_0 and L'_1, respectively. The shift factors for the storage moduli master curves were found to fit well to the WLF equation, and the fittings yielded comparable parameters in the temperature range from −10 to 30 °C. For the storage moduli curves, the fitting of the WLF equation with the shift factors for L'_0 system gave C_1 and C_2 as 11 and 73, respectively. For L'_1, the fittings yielded $C_1 = 10$ and $C_2 = 47$. These parameters are similar to those of L'_0 system. The results suggest that the viscoelastic responses for FKM/ACM and 20% LCP blend as described by the WLF equation were similar.

Information on the dynamic free volume characteristics of the samples was deduced from the following relations [13]:

$$C_1 = B/2.3f_0 \tag{2}$$

$$C_2 = f_0/\alpha_f \tag{3}$$

$$C_1C_2 = B/2.3\alpha_f \tag{4}$$

f_0 is fractional free volume at T_0, α_f is the coefficient of thermal expansion of the fractional free volume and B is numerical constant, usually taken equal to unity. For both L'_0 and L'_1 samples, the calculated fractional free volume ($10^2 \times f_0$) using above relations are 4.83 and 3.9, respectively. The thermal expansion coefficient ($10^3 \times \alpha_f$), 0.88 and 0.63 have been calculated for L'_0 and L'_1.

From the above results it was found that the addition of LCP to FKM/ACM system decreased of both f_0 and α_f.

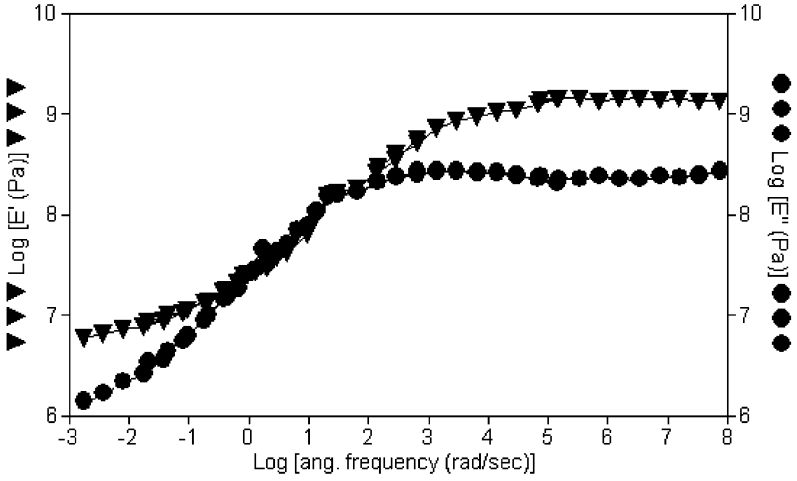

Fig. 11. Master curves generated by shifting the storage and loss modulus curves of L'_1 blend according to the time–temperature principle.

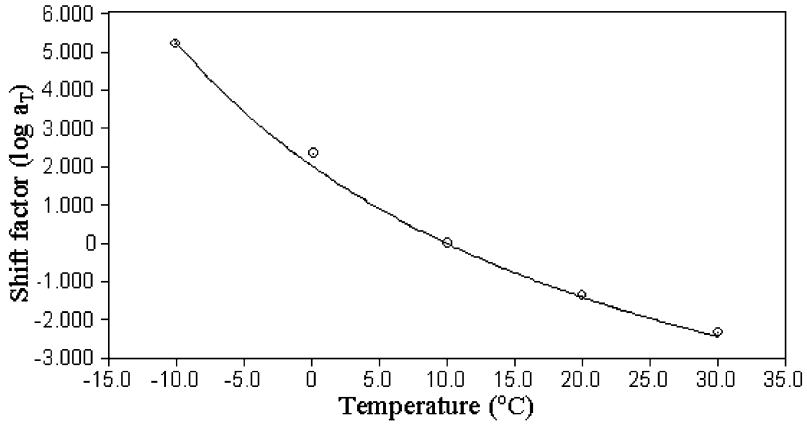

Fig. 12. WLF fittings of the shift factors obtained by shifting both the storage and loss modulus curves for the FKM/ACM blend.

Therefore this result showed that the addition of LCP induced some reduction in the dynamic free volume in the FKM/ACM blend.

The activation energy, E_a, was calculated by assuming an Arrhenius dependence of the shift factors [30,31];

$$\log a_T = \frac{E_a}{R(1/T - 1/T_0)} \tag{5}$$

The Arrhenius theory treated the shift factors as transition states with characteristic activation energy. The activation energies, however, may vary as a function of temperature [31]. In our analysis, the activation energy was calculated at three different temperatures (reference temperatures) in the glass transition region and the values were represented in Table 3, which clearly indicated that the activation energies of the shift factors in the glass transition region increased with increasing the temperature. The FKM/ACM blend showed the activation energies comparatively higher than the activation energy of 20% LCP filled FKM/ACM. The activation energies for both the systems found in the range of 190–275 kJ mol^{-1}. For glass transition, it is not unusual to find activation energies 190–275 kJ mol^{-1}, greater than the energy of a primary chemical bond. Clearly such large activation energies indicated that there was a high degree of complexity in the motion associated with the relaxations. This impression of complexity is confirmed by large activation entropies for these relaxations. The activation entropy (ΔS^*) was derived from the relationship proposed by Starkweather [32]:

$$\Delta S^* = E_a - RT_0[1 + \ln(kT_0/2\pi h)] \tag{6}$$

Where R, k, and h are the gas constant, Boltzmann's constant and Planck's constant, respectively, and T_0 is the characteristic temperature relative to the reference frequency of 1 Hz. The activation entropy at the beginning, middle part and end of the E'' peak for both L'_0 and L'_1 were listed in Table 3. The ΔS^* values can be considered as an indication of motional cooperativity. Values of the order of 650 J K^{-1} mol^{-1} or larger are observed in the central and high-temperature parts of the E'' peak of the LCP unfilled FKM/ACM blend. They correspond to a rather high motional cooperativity. On the other hand, small ΔS^* values (550 J K^{-1} mol^{-1} or less) are observed in the LCP filled FKM/ACM blend. They accounted for the hindrance of some of the cooperative motions.

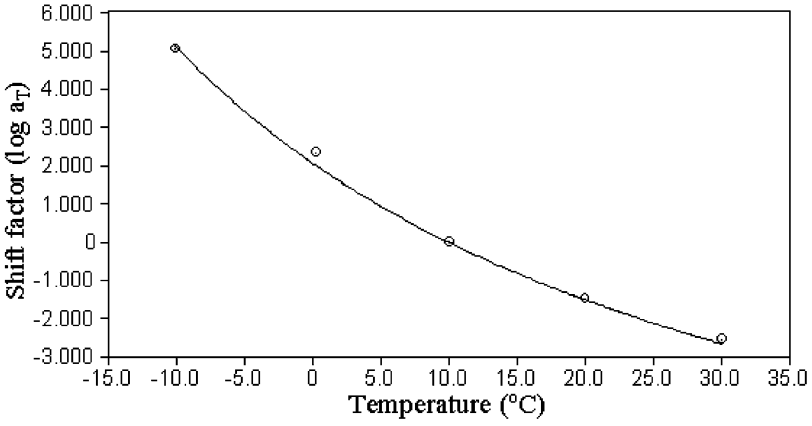

Fig. 13. WLF fittings of the shift factors obtained by shifting both the storage and loss modulus curves for the 20% LCP filled FKM/ACM blend.

Table 3
Activation energy and entropy of the blends at reference temperatures

	T_1 (K)	E_{a1} (kJ mol^{-1})	ΔS_1^* (J mol^{-1} K^{-1})	T_2 (K)	E_{a2} (kJ mol^{-1})	ΔS_2^* (J mol^{-1} K^{-1})	T_3 (K)	E_{a3} (kJ mol^{-1})	ΔS_3^* (J mol^{-1} K^{-1})
L'_0	263	210	552	283	252	646	303	275	661
L'_1	263	191	481	283	217	520	303	237	536

4. Conclusion

Viscoelastic properties of FKM, FKM/ACM and their blends were measured in dynamic mechanical experiments. Storage modulus of the binary and ternary blends increased with LCP content due to high intrinsic modulus of LCP. The glass transition temperatures of the binary and ternary blends were shifted to higher temperature side with the addition of LCP due to decrease in the flexibility of molecular chains as increasing the LCP content in the blend. Simple horizontal shifts of the storage (E') and loss (E'') moduli curves seemed to indicate that TTS to hold good for both FKM/ACM and FKM/ACM/LCP blends. The WLF and Arrhenius equations were used to describe the shift factors obtained from multiple frequency experiments near the glass transition temperatures. The activation energies of the shift factors were found in the range of 190–275 kJ mol^{-1}, and these values were not unusual for glass transition. Viscoelastic relaxations of FKM/ACM and FKM/ACM/LCP had positive activation entropies, which were very large. In these cases, the activated state must be more disordered than the ground state, and the relaxations were believed to involve complex cooperative interactions among neighbouring groups.

Acknowledgements

Authors are thankful to Lady Davis fellowship, Israel for providing the facilities to carry out the work under the guidance of Prof M. Narkis of chemical engineering department, Technion, Haifa-32000, Israel.

References

[1] Jackson WJ, Kuhfuss HF. J Polym Sci Chem 1976;14:2043.
[2] Brostow W. Polymer 1990;31:979.
[3] Jakobson EE, Faitelson LA, Kulichikhin VG. Mech Compos Mater 1991;27:514.
[4] Zulle B, Demarmels A, Plummer CJG. Polymer 1992;34:3628.
[5] Plummer CJC, Wu Y, Davies P. J Appl Polym Sci 1993;48:731.
[6] Plummer CJC, Zulle, Demarmels A. J Appl Polym Sci 1993;48:751.
[7] Buijs JAHM, Vroege GJ. Polymer 1993;34:4692.
[8] Brostow W, Hess M, Lopez BL. Macromolecules 1994;27:2262.
[9] Siegmann A, Dagan A, Kenig S. Polymer 1985;26:1325.
[10] Joseph E, Wilkes GL, Baird DG. Polym Eng Sci 1985;25:377.
[11] Shih CK. Polym Eng Sci 1976;16:328.
[12] Brostow W, D'Souza NA, Kubat J, Maksimov RD. Mechanical and thermophysical properties of polymer liquid crystals. 1st ed. London: Chapman and Hall; 1998 [chapter 12].
[13] Ferry JD. Viscoelastic properties of polymers. 3rd ed. New York: Wiley; 1980 [chapters 11 and 12].
[14] Hatzikiriakos S. Polym Eng Sci 2000;40:2279.
[15] Rosati D, Van Loon B, Navard P. Polymer 2000;41:367.
[16] Li R. Mater Sci Eng 2000;A278:36.
[17] McCrum NG. J Polym Sci 1958;27:555.
[18] McCrum NG. J Polym Sci 1959;34:355.
[19] McCrum NG. Macromol Chem 1958;34:50.
[20] Paul DR, Newman S. Polymer blends. vol. 1. New York: Academic Press; 1978 [chapter 8].
[21] Mark Hoffman D. Polym Eng Sci 2003;43:139.
[22] Da Silva L, Bretas RES. Polym Eng Sci 2000;40:1414.
[23] Decarvalho B, Bretas RES. J Appl Polym Sci 1995;33:1259.
[24] Weiss RA, Huh W, Nocolais L. Polym Eng Sci 1987;27:684.
[25] Fowkes FM, Tichler DO, Lannigan JA, John CMA, Halliwell MJ. J Polym Sci, Polym Chem Ed 1984;22:547.
[26] Zhang H, Weiss RA, Kuder JE, Cangiano D. Polymer 2000;41:3069.
[27] Kohli A, Chung N, Weiss RA. Polym Eng Sci 1989;29:573.
[28] Chakraborty S, Sahoo NG, Jana GK, Das CK. J Appl Polym Sci 2004;93:711.
[29] Nielsen LE, Landel RF. Mechanical properties of polymers and composites. 2nd ed. New York: Marcel Dekker; 1994. p. 491–2.
[30] Williams ML, Landel RF, Ferry JD. J Am Chem Soc 1955;77:3701.
[31] Ward IM. Mechanical properties of solid polymers. 2nd ed. New York: Wiley; 1979 [chapter 7].
[32] Starweather HWJ. Macromolecules 1981;14:1277.